Available online at www.sciencedirect.com
ScienceDirect
Trans. Nonferrous Met. Soc. China 22(2012) 1686−1692
Transactions of Nonferrous Metals Society of China
www.tnmsc.cn

Microstructure and properties of Al/Si/SiC composites for electronic packaging

ZHU Xiao-min, YU Jia-kang, WANG Xin-yu

State Key Laboratory of Solidification Processing, Northwestern Polytechnical University, Xi'an 710072, China

Received 11 July 2011; accepted 8 October 2011

Abstract: The Al/Si/SiC composites with medium volume fraction for electronic packaging were fabricated by gas pressure infiltration. On the premise of keeping the machinability of the composites, the silicon carbide particles, which have the similar size with silicon particles (average 13 μm), were added to replace silicon particles of same volume fraction, and microstructure and properties of the composites were investigated. The results show that reinforcing particles are distributed uniformly and no apparent pores are observed in the composites. It is also observed that higher thermal conductivity (TC) and flexural strength will be obtained with the addition of SiC particles. Meanwhile, coefficient of thermal expansion (CTE) changes smaller than TC. Models for predicting thermal properties were also discussed. Equivalent effective conductivity (EEC) was proposed to make H−J model suitable for hybrid particles and multimodal particle size distribution.
Key words: Al/Si/SiC composite; electronic packaging; thermal properties; flexural strength

1 Introduction

With the rapid development of electronic industry, component size reduction and computing capability increase, 30% of current chip performance was limited by packaging materials [1]. It poses as an urgent issue to find new materials with superior properties. However, copper suffers from a high coefficient of thermal expansion (CTE), while Fe−Ni alloy is very poor in thermal conductivity (TC) [2]. The properties of traditional materials, such as W/Cu and Mo/Cu, are insufficiently high with respect to the predicted exponential growth of power density in electronic packaging [3]. In fact, these traditional materials, despite featuring a low CTE mismatch, are heavy and difficult to form. Many kinds of new electronic packaging materials have appeared and composites are becoming the primary choice.

Owning to their excellent mechanical capacity, metal matrix composites were expected as the potential packaging materials. Particulate-reinforced aluminum matrix composites, which have low and designable thermal expansion properties, excellent thermal conductivity and low density, have been attached much importance. Al/Si composites are attractive materials with many outstanding properties, including higher thermal conductivity, lower coefficient of thermal expansion and low density [4−6]. Compared with Al/SiC [7,8] and Al/diamond [9−11], Al/Si composites reinforced with fine particles have lower CTE and better machinability. However, the strength of the Al/Si composites is lower, and thermal conductivity, especially reinforced with fine particles, is low. The addition of SiC was expected to enhance the thermal conductivity and flexural strength [12,13].

There have been many models for predicting thermal properties, including Turner [14] and Kerner [15] models for CTE, Hasselman−Johnson (H−J) model [16] for TC. The H−J model was widely used due to the introduction of interfacial thermal conductivity. But just like many other predictive schemes for composites with single reinforcing phase or monomodal particle size, composites reinforced with hybrid particles and bimodal particle size become more and more extensively used in recent years, and what we demand most now is to develop a new predicting model for composites reinforced with hybrid particles and bimodal particle size distribution. An improved H−J model was used in this work. It would apply for hybrid and bimodal particle size distribution. In addition, Turner and Kurner models are always reported to predict CTE of composites, like

Foundation item: Project (60776019) supported by the National Natural Science Foundation of China; Project (61-TP-2010) supported by the Research Fund of the State Key Laboratory of Solidification Processing (NWPU), China
Corresponding author: YU Jia-kang; Tel: +86-29-88494987; E-mail: jkyu@nwpu.edu.cn
DOI: 10.1016/S1003-6326(11)61374-5

Al/SiC, Al/diamond or Cu/diamond composites. However, little work has been done on Al/Si composites, especially with hybrid irregular particles. Thus, it would be an important work to get to know the feasibility of the Turner and Kerner models, and H−J model for predicting thermal properties of composites with hybrid irregular particles.

Gas pressure infiltration is more favorable than squeeze casting with respect to interfacial bonding and thermal properties of the composites. The process is a low cost and simple technology, by which dense, uniformly distributed and continuous composites can be fabricated [17].

The objective of this work is to investigate the influence of SiC addition on the properties of the Al/Si composites. It is expected that the thermal and mechanical properties of the Al/Si composites would be enhanced by the addition of SiC particles without reducing the machinability of the composites. Models for predicting thermal properties are also discussed in this paper.

2 Experimental

2.1 Materials and methods

A356(Al−7Si−0.3Mg) aluminum alloy was used as a matrix material, and silicon particles with an average size of 13 μm were used in this work. In order to enhance the mechanical and thermal properties, powders were mixed with the same total volume fraction containing 0, 4%, 8% and 12% of silicon carbide particles, which has a similar particle size with silicon particles. Silicon particles with different ratios of silicon carbide particles were mixed for about 30 min in the ball mill. Oleic acid, beewax and ceresin wax were added to mix uniformly, and then handed in a boat with special shape. De-waxing and fritting were carried out in a sintering furnace for about 12 h at a special heating temperature.

Infiltration was carried out in a pressure infiltration apparatus shown in Fig.1. The temperatures of the lower and upper furnace were 800 °C and 750 °C respectively. Vacuum was applied until a pressure of 4 kPa was reached before heating, then the melted aluminum alloy was pressurized into the preform. Solidification of the aluminum alloy occurred right away.

2.2 Characterization

The microstructure of the composites was observed by Olmpus MPG4. The fracture morphology was observed by Tescan Vega scanning electron microsope. A Philips X' Pert MPD Pro X-ray diffraction (XRD) was applied to investigating the phase composition of the oxidized silicon and silicon carbide particles. The flexural strength was obtained by three-point bending using Instron 3382 electronic multi-purpose testing machine, with a span of 30 mm in length, and a punch velocity of 0.05 mm/min. The CTE was measured on a DIL 402C dialmeter (NETZSCH Crop.) with a heating rate of 5 °C/min in the temperature range of 30−100 °C and an argon atmosphere with a flowing rate of 50 mL/min used to keep the chamber temperature constant. The flexural and CTE samples were in rectangles with dimensions of 40 mm×4 mm×4 mm and 25 mm×4 mm×4 mm, respectively. The thermal conductivity (TC) was calculated from the measured thermal diffusivity determined by LFA457 laser flash method (the method was described in detail in Refs. [18,19]), the measured density, and an estimated value of the specific heat of the composites. The sample for thermal diffusivity measuring was a disk with a diameter of 12.7 mm and a thickness of 3 mm. The results represent the average of three tests in most cases. The errors for all the volume fractions are ±1%.

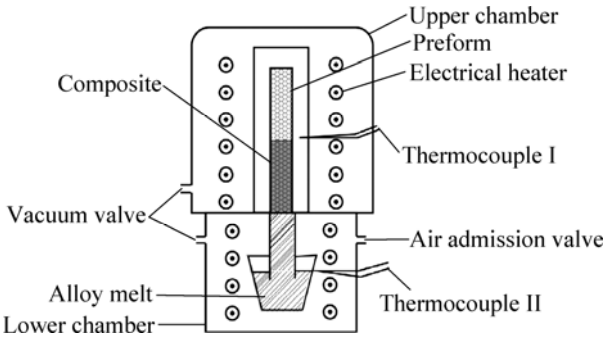

Fig. 1 Schematic diagram of gas pressure infiltration apparatus

3 Results and discussion

3.1 Microstructure and flexural strength

The representative morphologies of Al/Si/SiC composites are shown in Fig. 2. The composites are all dense and macroscopically homogeneous. Excellent thermal and mechanical properties would be expected due to the dense, uniform microstructure.

Figure 3 shows the fracture surface of the composites. The main fracture mechanism of the composites was ductile fracture of the aluminum matrix. According to Griffith's theory, the particle is considered to be broken if the stress in the particle exceeds the Griffith criterion: $\sigma_c^p = k_c^p / \sqrt{d}$, where k_c^p is a constant related to the fracture toughness of the particles together with geometrical factors and σ_c^p is the fracture stress of particles with diameter of d. It can be rationalized that large silicon particles have a lower fracture stress and are prone to cracking. Large particles with pre-existing microcracks will also lower the flexural strength of the composites. Furthermore, small silicon particles have a lower chance of defects and cracks than

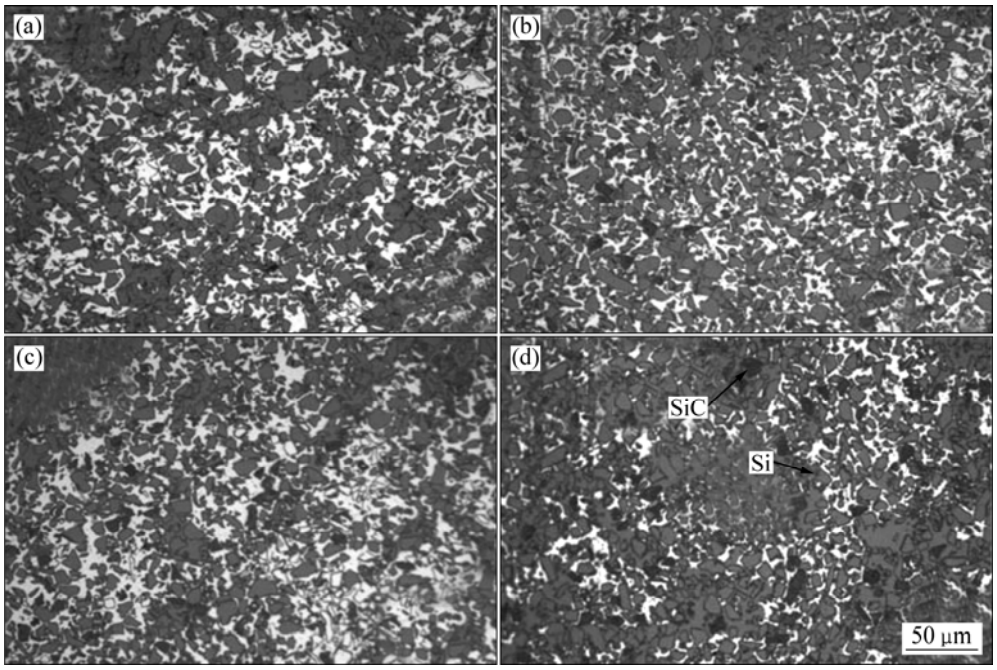

Fig. 2 SEM images of Al/Si/SiC with different SiC volume fractions: (a) 0; (b) 4%; (c) 8%; (d) 12%

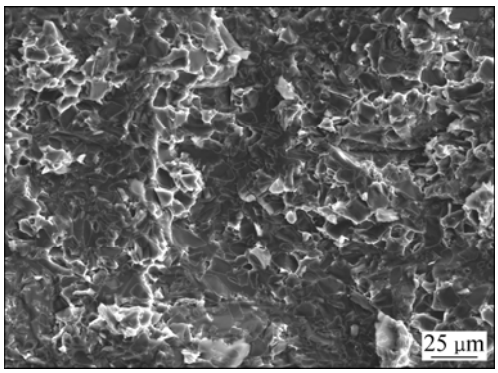

Fig. 3 SEM image showing fracture micrograph of Al/Si/SiC

large particles [20,21]. In the study of FLOM and ARSENAULT [22], little particle fracture would be found when the particle size was less than 20 μm. There are a smaller amount of particles which are over 20 μm in size. SiC has higher strength than silicon and both SiC and Si are bonded with aluminum matrix by SiO_2 (Fig. 4), which generated in the process of sintering. Thus, extremely individual brittle fracture of Si particles, not SiC particles was observed on the fracture surface.

Figure 5 shows the flexural strength of composites versus SiC volume fraction. From the results given in Fig. 5, the addition of SiC can apparently enhance the flexural strength of Al/Si composites. SiC has higher strength and rigidity than silicon. Silicon carbide particles have higher elastic modulus than silicon particles. Silicon carbide particles can lead to an adjustment of the stress in the reinforcements compared with the stress distribution of Al/Si. Silicon carbide particles with higher elastic modulus will bear a higher load and lower the stress in silicon particles. Meanwhile, silicon carbide particles have similar size with silicon particles, and little distortion may be observed. The above-mentioned reasons lead to the higher flexural strength of the composites.

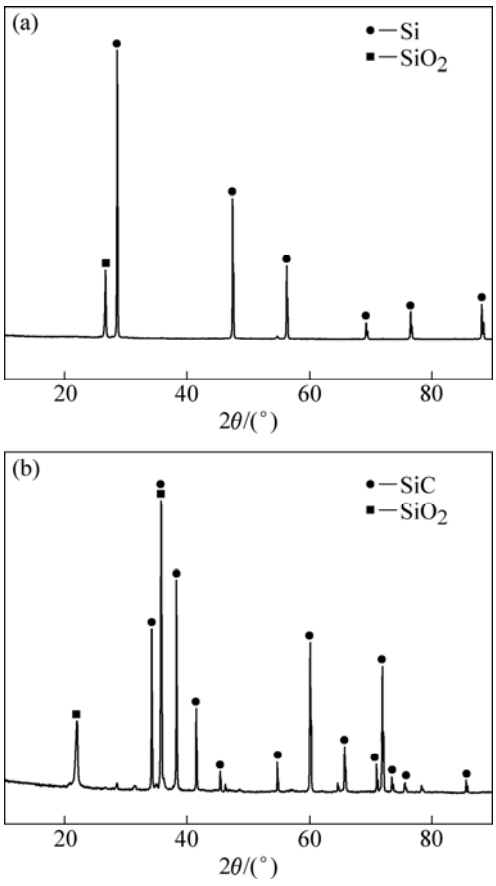

Fig. 4 XRD patterns of particles: (a) Si; (b) SiC

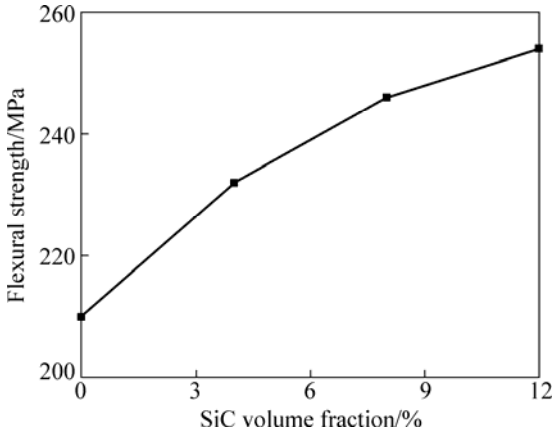

Fig. 5 Flexural strength of Al/Si/SiC versus SiC volume fraction

3.2 Coefficient of thermal expansion

Figure 6 shows the CTE of composites with different volume fractions of silicon carbide particles and the comparison between theoretical predictions and experimental data. The CTE is not linearly changed with increasing the volume fraction of silicon carbide particles. It is shown that the CTE of the composites has a smaller-scale increase with the addition of silicon carbide particles. Silicon carbide has higher CTE than silicon, as shown in Table 1. Few defects were observed as a result of similar size for two kinds of particles. Owning to the above reasons, a smaller-scale increase of CTE was obtained by the addition of SiC, which would not affect the applications of the composites.

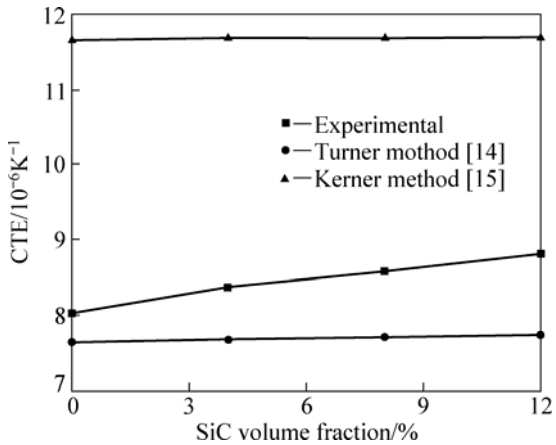

Fig. 6 CTEs of Al/Si/SiC composites and comparison between theoretical predictions and experimental data versus SiC volume fraction

TURNER [14] and KERNER [15] models were used to calculate theoretical CTE of the composites. CTE of the composites can be derived from Eq. (1) and Eq. (2) by Turner and Kerner methods relatively.

$$\alpha_c = \frac{\sum \alpha_i K_i \varphi_i}{\sum K_i \varphi_i},\ i=1,\ 2,\ 3 \tag{1}$$

where K, α, φ and i are the bulk modulus, CTE, volume fraction, and different phase, respectively.

$$\begin{cases} \alpha_c = \Sigma \alpha_i \varphi_i + \dfrac{4G_1}{K_c}\left[\sum \dfrac{K_c - K_i}{4G_1 + 3K_i}(\alpha_1 - \alpha_i)\varphi_i\right] \\ K_c = \sum K_i \varphi_i, i = 1, 2, 3 \end{cases} \tag{2}$$

where G_1 is the shear modulus of the matrix; K_c is the bulk modulus of the composites; α_c is the CTE of composites.

The parameters used for predictions are shown in Table 1. It could be seen in Fig. 6 that both models are not in good agreement with the experimental data. The predicted data by Turner model are far lower than experiment data. Turner model only contains material under isopressing, while the internal stress in real material is far more complicated, and furthermore, Turner model also neglects the internal stress generated in the cooling process. Kerner model considers both normal and shearing stresses, but the calculated CTE is much higher than experimental ones. This may be attributed to the fact that the particle shape and residual stress in the composites were not considered in Kerner model. A spherical assumption for reinforcing particles was made in Kerner model. However, both silicon and SiC particles have irregular shapes which would introduce more complicated stress in composites compared with spherical particles. Residual stress in the composites introduced by the CTE mismatch between the matrix phase and reinforcing phase was another stress which prevents the expansion of the metal matrix. The effect of particle size has been out of consideration in both models. Meanwhile, both two models predict that CTEs of the composites increased slower with the volume fraction of silicon carbide particles than the experimental ones. Thus, the general range of CTE can be determined by the two models, but it is not credible to use the two models to predict accurately the CTE of the Al/Si/SiC composites.

Table 1 Parameters of Al, Si and SiC

Material	$\alpha/10^{-6}K^{-1}$	K/GPa	G/GPa
Al	22.1	68.55	26.6
Si	4.2	235	−
SiC	4.6	227.3	−

3.3 Thermal conductivity

The thermal conductivity of composites is mainly governed by the thermal conductivity of each component,

their volume fraction, shape and size of the inclusion phase, as well as their interfacial condition. The thermal diffusivity of the composites was investigated by laser flash method and the density of the composites was examined by the Archimedes method. The density and specific heat capacity of the composite material can be calculated from Eqs. (3) and (4) respectively.

$$\rho_{\text{theot}} = \rho_{\text{Si}}\varphi_{\text{Si}} + \rho_{\text{SiC}}\varphi_{\text{SiC}} + \rho_{\text{Al}}\varphi_{\text{Al}} \quad (3)$$

$$c_{\text{theor}} = (c_{\text{Si}}\varphi_{\text{Si}}\rho_{\text{Si}} + c_{\text{SiC}}\varphi_{\text{SiC}}\rho_{\text{SiC}} + c_{\text{Al}}\varphi_{\text{Al}}\rho_{\text{Al}})/\rho_{\text{theor}} \quad (4)$$

where ρ_{Si}=2.33 g/cm^3, ρ_{SiC}=3.21 g/cm^3 and ρ_{Al}=2.68 g/cm^3, are the densities of silicon, silicon carbide and AlSi7 alloy respectively; φ_{Si} is the volume fraction of silicon; c_{Si}=0.7 J/(g·K), c_{SiC}=0.66 J/(g·K) and c_{Al}=0.88 J/(g·K), are the specific heat capacities of silicon, silicon carbide and AlSi7 alloy, respectively. The thermal conductivity could be calculated according to the following formula:

$$k = \alpha c_{\text{theor}}\rho \quad (5)$$

where α, c_{theor}, ρ and k are the coefficients of thermal diffusion, calculated specific heat capacity, density and thermal conductivity for Al/Si/SiC composites, respectively.

The improved H−J model was used to account for composites with two different phase distributions. The equations of H−J model are as follows:

$$K_{\text{p}}^{\text{eff}} = \frac{K_{\text{p}}}{1 + 2K_{\text{p}}/(hd)} \quad (6)$$

where K_{p} is the intrinsic thermal conductivity of the disperse (inclusion) particles; d is the average diameter of particles; h is the intrinsic interfacial thermal conductivity. As mentioned previously, the H−J model can be implemented to calculate the thermal conductivity of PMCs with interfacial thermal resistance, according to the following equation:

$$K_{\text{c}} = \frac{K_{\text{m}}[2K_{\text{m}} + K_{\text{p}}^{\text{eff}} + 2(K_{\text{p}}^{\text{eff}} - K_{\text{m}})\varphi_{\text{p}}]}{2K_{\text{m}} + K_{\text{p}}^{\text{eff}} - (K_{\text{p}}^{\text{eff}} - K_{\text{m}})\varphi_{\text{p}}} \quad (7)$$

where K is the thermal conductivity; φ is the volume fraction of inclusions, and the subscripts c, m and p refer to composite, matrix and reinforcement particles, respectively. H−J model has been proved to be a simple and powerful approach in describing the conductive properties of composites with an imperfect interface when particles and matrix exhibit a low ratio of conductivities. However, the model can only been applied to composites with single reinforcing phase and a monomodal particle size distribution, not been used for hybrid particles and multimodal particle size distribution.

To solve this problem, an equivalent effective conductivity(EEC) is proposed in this contribution, according to the following equation:

$$\overline{K}_{\text{p}}^{\text{eff}} = \frac{\sum K_{\text{p}i}^{\text{eff}}\varphi_{\text{p}i}}{\sum \varphi_{\text{p}i}} \quad (8)$$

where $\varphi_{\text{p}i}$ is the volume fraction of different reinforcing particles or the particles with different sizes ($\sum \varphi_{\text{p}i} = \varphi_{\text{p}}$).

Then adding $\overline{K}_{\text{p}}^{\text{eff}}$ to Eq. (7), the predicted thermal conductivity would be obtained. With the help of the equivalent effective conductivity (EEC), thermal conductivity of the composites with hybrid particles or multimodal particle size distribution would be predicted by the H−J model.

It is assumed that the thermal conductivities of the AlSi7 matrix, the SiC and the silicon particles are 170 W/(m·K) [23], 203 W/(m·K) [24] and 150 W/(m·K) [6] respectively, in order to obtain the uncertain parameters. The interfacial thermal conductivities, h, may be estimated with various models and the simplest one is the acoustic mismatch model [25]. This model treats the interface heat transfer in terms of continuum mechanics by calculating the probability of an incident phonon to pass the interface, and h is calculated to be:

$$h \cong \frac{1}{2}\rho_1 c_p \frac{c_1^3\rho_1\rho_2 c_1 c_2}{c_2^2(\rho_1 c_1 + \rho_2 c_2)^2} \quad (9)$$

where c_p is the specific heat capacity of metal; ρ is the density; c is the phonon velocity; subscripts 1 and 2 refer to metal and reinforcement, respectively.

Taking ρ_1=2700 kg/m^3, c_p=895 J/(kg·K), and c_1=3595 m/s [25] for the metal (considered here pure aluminum, given the lack of data for Al−Si alloys), and ρ_2=3210 kg/m^3, 2330 kg/m^3 for SiC and silicon, respectively, c_2=11600 m/s, 8970 m/s for SiC and silicon particles [25], respectively, we obtain h=6.7×10^7 W(m^2·K) and 9.1×10^7 W(m^2·K) for SiC and silicon, respectively. Figure 7 shows the results of the thermal conductivities of the composites as the function of SiC addition fraction according to both experiment and prediction by H−J model. On the premise of the same volume fraction of reinforcing particles, composites with the addition of SiC particles have higher thermal conductivity than the composites with pure silicon particles. Thermal conductivity increases with the addition of SiC particles. Its thermal conductivity was increased by about 10% while the volume fraction of SiC particles was 12%. Silicon carbides have higher thermal conductivity than silicon particles, and silicon carbide particles have similar size with silicon particles, and little distortion, which would offer resistance to the lattice vibrations and motions of free electrons. Meanwhile, there were few pores in the composites, which is another

influencing factor to the thermal conductivity. The above mentioned reasons lead to the increase of thermal conductivity with the addition of silicon carbide particles.

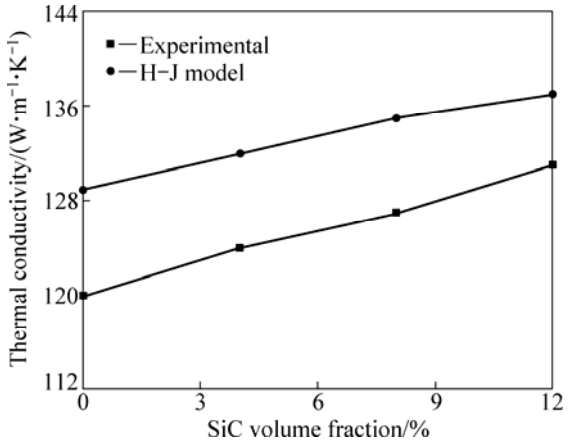

Fig. 7 Experimental data of thermal conductivity and ones predicted by H−J model as function of volume fraction of SiC

The predicted result by the H−J model is also shown in Fig. 7. The predicted results are in good agreement with the experimental data. Size, volume fraction, mismatch between matrix and reinforcement and interfacial thermal resistance etc. were all in consideration in H−J model. It was proved to be in good agreement with the experimental data for predicting thermal conductivity of the composites with single reinforcing phase and monomodal particle size distribution. With the help of EEC, thermal conductivity of the composites with hybrid reinforcing particles or multimodal particle size distribution could be obtained by the H−J model. Meanwhile, there is a little difference between experimental and predicted result. This may be related to the influence of SiO_2 generated in the process of sintering and on the assumption of spherical particles.

4 Conclusions

1) The Al/Si/SiC composites with medium volume fraction and fine particle size were fabricated by gas pressure infiltration. The composites were all dense and macroscopically homogeneous. The main fracture mechanism of the composite is matrix ductile fracture, extremely individual brittle fracture of silicon particles was observed on the fracture surface. Both SiC and silicon are bonded with aluminum matrix by SiO_2, which generates in the process of sintering. The SiO_2 would improve the interfacial bonding strength.

2) With the addition of fine SiC particles, thermal and mechanical properties are highly improved. On the premise of keeping the machinability of the composites, flexural strength and thermal conductivity of the composites are increased with increasing SiC particles. Meanwhile, the coefficient of thermal expansion changes relatively small. The general range of CTE can be determined by Turner and Kerner models, but it is not credible to use these two models to predict accurately the CTE of the Al/Si/SiC composites.

3) The predicted results by H−J models are in good agreement with the experimental data. With the help of proposed EEC, thermal conductivity of the composites with hybrid particles or multimodal particle size distribution can be predicted by the H−J model.

References

[1] GERMAN R M, HENS K F, JOHNSON J L. Powder metallurgy processing of thermal management materials for microelectronic applications [J]. Int J Powder Metall, 1994, 30: 205−214.

[2] CHUNG D D L. Materials for thermal conduction [J]. Appl Therm Eng, 2001, 21(16): 1593−1605.

[3] ZWEBEN C. Advances in composite materials for thermal management in electronic packaging [J]. JOM, 1998, 50(6): 47−51.

[4] XIU Zi-yang, ZHANG Qiang, SONG Mei-hui. Microstructure and properties of Sip/4023Al composites [J]. Transactions of Nonferrous Metals Society of China, 2005, 15(s3): s115−s117.

[5] XIU Zi-yang, WU Gao-hui, ZHANG Qiang. Thermo-physical properties of Sip/LD11 composites for electronic packaging [J]. Transactions of Nonferrous Metals Society of China, 2005, 15(s2): s227−s230.

[6] CHIEN C W, LEE S L, LIN J C. Processing and properties of high volume fraction aluminum/silicon composites [J]. Mater Sci Technol, 2003, 19: 1231−1234.

[7] CHU Ke, JIA Cheng-chang, LIANG Xue-bing, CHEN Hui, GUO Hong. The thermal conductivity of pressure infiltrated SiCp/Al composites with various size distributions: Experimental study and modeling [J]. Mater Des, 2009, 30: 3497−3503.

[8] NAM T H, REQUENA G, DEGISCHER P. Thermal expansion behavior of aluminum matrix composites with densely packed SiC particles [J]. Compos Part A, 2008, 39: 856−865.

[9] XUE C, YU J K, ZHU X M. Thermal properties of diamond/SiC/Al composites with high volume fractions [J]. Mater Des, 2011, 32: 4225−4229.

[10] FENG H, YU J K, TAN W. Microstructure and thermal properties of diamond/aluminum composites with TiC coating on diamond particles [J]. Mater Chem Phys, 2010, 124: 851−855.

[11] YANG Bo, YU Jia-kang, CHEN Chuang. Microstructure and thermal expansion of Ti coated diamond/Al composites [J]. Transactions of Nonferrous Metals Society of China, 2009, 19(5): 1167−1173.

[12] ZHANG Qi-guo, ZHANG Hong-xiang, GU Ming-yuan. Studies on the fracture and flexural strength of Al/Sip composite [J]. Mater Letter, 2004, 58: 3545−3550.

[13] ZHANG Qi-guo, GU Ming-yuan. Effect of silicon carbide particles on properties of Al/Sip + SiCp [J]. Mater Sci Eng A, 2006, 419: 86−90.

[14] TURNER P S. Thermal-expansion stresses in reinforced plastics [J]. J Res NBS, 1946, 37: 239−250.

[15] KERNER E H. The elastic and thermo-elastic properties of composite media [J]. Proc Phys Soc B, 1956, 69: 808−813.

[16] HASSELMAN D P H, JOHNSON L F. Effective thermal conductivity of composites with interfacial thermal barrier resistance

[J]. J Compos Mater, 1987, 21: 508−515.
[17] MOLINA J M, SARAVANAN R A, ARPON R. Pressure infiltration of liquid aluminium into packed SiC particulate with a bimodal size distribution [J]. Acta Mater, 2002, 50: 247−257.
[18] YAMAMOTO Y, IMAI T, TANABE K, TSUNO T, KUMAZAWA Y, FUJIMORI N. The measurement of thermal properties of diamond [J]. Diamond Relat Mater, 1997, 6: 1057−1061.
[19] TWITCHEN D J, PICKLES C S J, COE S E, SUSSMANN R S, HALL C E. Thermal conductivity measurements on CVD diamond [J]. Diamond Relat Mater, 2001, 10: 731−735.
[20] CHEN Hang-yon, CHAO Chuen-guang. Effect of particle-size distribution on the properties of high volume-fraction SiCp-Al-based composites [J]. Metall Mater Trans A, 2000, 31: 2351−2359.
[21] NAN C W, CLARK D R. The influence of particle size and particle fracture on the elastic/plastic deformation of metal matrix composites [J]. Acta Mater, 1996, 44: 3801−3811.
[22] FLOM Y, ARESENAULT R J. Effect of particle size on fracture toughness of SiC/Al composite materials [J]. Acta Mater, 1989, 37: 2413−2423.
[23] JOSEPH R D, PENELOPE A, STEVEN R L. Metals handbook [M]. 10th ed. OH: ASM International, 1979.
[24] MOLINA J M, NARCISO J, WEBER L. Thermal conductivity of Al−SiC composites with monomodal and bimodal particle size distribution [J]. Mater Sci Eng A, 2008, 480: 483−488.
[25] SWARTZ E T, POHL R O. Thermal boundary resistance [J]. Rev Mod Phys, 1989, 61: 605−611.

电子封装用 Al/Si/SiC 复合材料的显微组织与性能

朱晓敏，于家康，王新宇

西北工业大学 凝固技术国家重点实验室，西安 710072

摘　要：采用气压浸渗法制备中体积分数电子封装用 Al/Si/SiC 复合材料。在保证加工性能的前提下，用与 Si 颗粒相同尺寸(13 μm)的 SiC 替代相同体积分数的硅颗粒制得复合材料，并研究其显微组织与性能。结果显示，颗粒分布均匀，未发现明显的孔洞。随着 SiC 的加入，强度和热导率将得到明显提高，但热膨胀系数变化较小，对使用影响也不大。讨论几种用于预测材料热学性能的模型。新的当量有效热导被引入后，H–J 模型将适用于混杂和多颗粒尺寸分布的情况。

关键词：Al/Si/SiC 复合材料；电子封装；热学性能；抗弯强度

(Edited by YANG Hua)